

Control of chaos in excitable physiological systems: A geometric analysis

David J. Christini and James J. Collins

Department of Biomedical Engineering, Boston University, 44 Cummings Street, Boston, Massachusetts 02215

(Received 11 April 1997; accepted for publication 9 July 1997)

Model-independent chaos control techniques are inherently well-suited for the control of physiological systems for which quantitative system models are unavailable. The proportional perturbation feedback (PPF) control paradigm, which uses electrical stimulation to perturb directly the controlled system variable (e.g., the interbeat or interspike interval), was developed for excitable physiological systems that do not have an easily accessible system parameter. We develop the stable manifold placement (SMP) technique, a PPF-type technique which is simpler and more robust than the original PPF control algorithm. We use the SMP technique to control a simple geometric model of a chaotic system in the neighborhood of an unstable periodic orbit (UPO). We show that while the SMP technique can control a chaotic system that has UPO dynamics which are characterized by one stable manifold and one unstable manifold, the success of the SMP technique is sensitive to UPO parameter estimation errors. © 1997 American Institute of Physics.

[S1054-1500(97)00504-1]

Deterministic chaos is characterized by dynamical behavior that appears to be random but actually is governed by a nonlinear deterministic system. Although chaos is unpredictable over long time periods, its deterministic nature often can be exploited by control techniques to obtain desired results. Chaos control techniques, which are “model-independent” because they do not require knowledge of a system’s underlying equations, have been applied successfully to a wide range of physical systems. Such success has fostered interest in applying model-independent control techniques to stabilize the fluctuations of excitable physiological systems, which are often well-understood qualitatively, but for which quantitative relationships between system components are usually incomplete. In this study, we use a geometric modeling analysis to demonstrate that model-independent control of excitable physiological systems is, in fact, dynamically feasible.

I. INTRODUCTION

Recent advances in the understanding of the dynamical mechanisms of physiological systems¹⁻⁶ have fostered interest in exploiting such mechanisms to control system behavior. Well-established model-based feedback control techniques utilize a system’s governing equations (i.e., an analytical system model) to control the dynamics of a system.⁷ Unfortunately, although many physiological systems are well-understood qualitatively, quantitative relationships between physiological system components are usually incomplete. Thus, because accurate analytical models cannot be developed for such systems, model-based control techniques are generally not applicable in physiological settings. Fortunately, for nonlinear dynamical systems, there is a new class of feedback control techniques, typically called *chaos control* techniques, that are model-independent, i.e., they do not require explicit knowledge of a system’s underlying

equations. Model-independent techniques extract necessary quantitative information from system observations and then use this extracted information to exploit the system’s inherent dynamics to achieve a desired control result. Thus, these techniques are inherently well-suited for the control of physiological systems. Here we use a geometric modeling analysis to examine the effectiveness of chaos control techniques for stabilizing excitable physiological systems.

II. OGY CHAOS CONTROL

In the seminal work in the area of model-independent feedback control, Ott, Grebogi, and Yorke (OGY)⁸ developed a control technique for chaotic dynamical systems. The OGY technique is based on the fact that the state point ξ of a chaotic system fluctuates continuously as it moves between infinitely many unstable periodic orbits (UPOs) embedded within the geometrically-finite state space known as the chaotic attractor. The goal of the OGY control technique is to stabilize the state point within one of these UPOs.

The OGY technique (see Fig. 1) exploits the fact that ξ always approaches the UPO $\xi^* = [x^*, x^*]^T$ (where superscript T denotes transpose and $[x^*, x^*]^T$ is a 2×1 column vector) along a characteristic path (the stable manifold) and departs from ξ^* along a different characteristic path (the unstable manifold). Although the system is nonlinear, the stable and unstable manifolds are linear in the neighborhood of ξ^* , where they can be approximated by the vectors e_s and e_u , respectively. Once ξ wanders into the neighborhood of the desired UPO (which is guaranteed because the chaotic attractor is ergodic), the OGY technique perturbs an accessible system parameter p by an amount δp such that ξ^* , e_s , and e_u are shifted to $\hat{\xi}^*$, \hat{e}_s , and \hat{e}_u , respectively. The resultant attracting force (due to \hat{e}_s) and repelling force (due to \hat{e}_u) move the state point from its current position ξ_n to its next position ξ_{n+1} . At the end of the current control cycle (i.e., when x is re-iterated and p is returned to its initial value), the

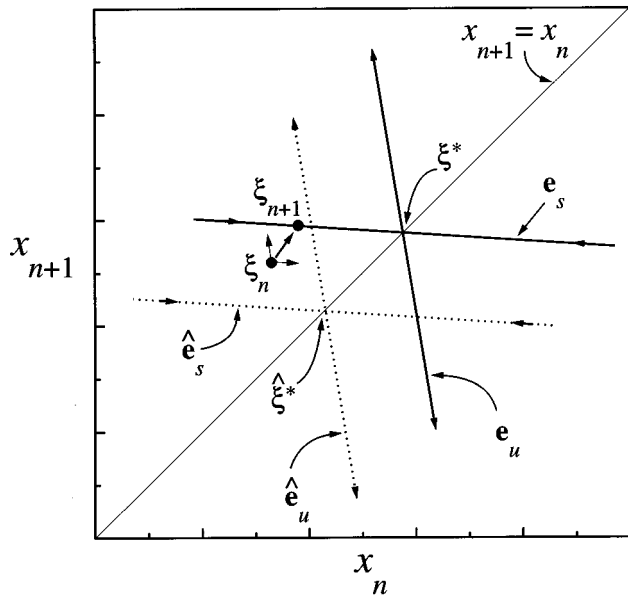


FIG. 1. Geometric depiction of the OGY control technique. A perturbation made to an accessible parameter shifts the UPO³³ ξ^* and its stable (e_s) and unstable (e_u) manifolds to $\hat{\xi}^*$, \hat{e}_s , and \hat{e}_u , respectively. The resultant attracting force (due to \hat{e}_s) and repelling force (due to \hat{e}_u) move the state point from its current position ξ_n to its next position ξ_{n+1} . At the end of the control perturbation (i.e., when the parameter is returned to its initial value), the UPO and manifolds return to their original locations, after which the state point ξ_{n+1} is located on e_s . The state point is subsequently attracted towards ξ^* via the stable manifold.

UPO and manifolds return to their original locations (ξ^* , e_s , and e_u). The key to the OGY technique is that δp is selected such that the relocated state point ξ_{n+1} lies on e_s . Following the control perturbation, the state point is subsequently attracted towards ξ^* via the stable manifold. Control is repeated at every iteration to prevent ξ_n from drifting away from ξ^* . Thus, the OGY parameter perturbations constrain the system's state point within the locally-linear UPO neighborhood by exploiting dynamics inherent to that UPO (specifically, the attracting property of the stable manifold). Importantly, ξ^* , e_s , e_u , and g are all estimated from past observations of the system. Thus, the OGY technique is practical from an experimental standpoint because it requires no analytical model of the system.

III. PPF-TYPE CONTROL OF EXCITABLE PHYSIOLOGICAL SYSTEMS

The OGY technique, and other similar model-independent chaos control techniques, have been applied to a wide range of physical systems, including magneto-elastic ribbons,⁹ electronic circuits,¹⁰ lasers,¹¹ chemical reactions,¹² driven single pendulums,^{13,14} and a driven double pendulum.¹⁵ The success of chaos control in stabilizing physical systems has fostered interest in applying these techniques to excitable physiological systems.^{16–22} In the first such application, Garfinkel *et al.*¹⁶ stabilized irregular cardiac rhythms in tissue from the interventricular septum of a rabbit heart. Unlike the physical systems controlled by the

OGY technique, no system parameter was readily-accessible for perturbation in the rabbit heart system. Garfinkel *et al.*¹⁶ therefore developed a technique known as *proportional perturbation feedback* (PPF) control, which is a modification of the original OGY technique. With PPF control, perturbations are made directly to the controlled system variable x [where x is an interbeat (cardiac) or interspike (neuronal) interval], rather than to a system parameter.^{23,24}

PPF control attempts to force the system's state point towards the UPO by placing it directly onto the stable manifold. This goal is accomplished by inducing premature beats via suprathreshold electrical stimulation, thereby shortening the expected value of x to a value which places it onto the stable manifold. The state point is subsequently attracted towards the UPO via the stable manifold. It is important to note that because suprathreshold electrical stimuli induce premature firings in excitable physiological systems (e.g., cardiac cells and neurons), control of this type cannot lengthen x . Thus, control stimuli can only be applied prior to long intervals.

In addition to the fact that the PPF control technique applies perturbations to the variable under control rather than to a system parameter, two other important differences — the frequency and size of perturbations — exist between the OGY and PPF control techniques. The OGY control technique exploits the exponential sensitivity of chaos to initial conditions by using only small perturbations to stabilize the desired UPO. However, because the exponential sensitivity causes rapid departure from the UPO, OGY perturbations must be applied at each Poincaré-map intersection to keep the system's state point from escaping from the UPO neighborhood. Similarly, the PPF control technique could, in principle, use frequent small perturbations (as often as every other beat)²⁵ to constrain the chaotic intervals within a small neighborhood around the UPO. However, such an approach is not ideal from a physiological perspective because a large percentage of action potentials would be stimulus-induced rather than spontaneous. Furthermore, such an approach would offer little perturbation-frequency improvement over traditional pacing techniques, such as demand pacing,²⁶ which do not attempt to exploit underlying system dynamics and therefore require frequent stimuli to achieve a desired control result. Thus, the preferable PPF-control approach is to allow the system's state point to wander away from the UPO along the unstable manifold until it reaches a maximum allowable distance (the *control threshold*) from the UPO. Once it crosses the control threshold, a PPF-interval perturbation (one which is large in comparison to the scale of perturbations required by OGY control) is introduced to force the state point onto the stable manifold. With this approach, PPF control uses relatively large, but infrequent, perturbations.

A. The PPF control technique

To place the system's state point onto the stable manifold of a UPO, the PPF control technique requires seven steps. Initially, the algorithm must estimate (from pre-

recorded data): **1)** The UPO ξ^* (see Refs. 27–30 for UPO-estimation methods and related techniques), **2)** the stable manifold e_s , **3)** the unstable manifold e_u , and **4)** the sensitivity of the UPO to perturbations:

$$g = \delta \xi^* / \delta x. \tag{1}$$

Then, at each control intervention [depicted geometrically in Fig. 2(a)], the algorithm must: **5)** Predict the next system value \hat{x}_{n+1} from x_n as:

$$\hat{x}_{n+1} = \lambda_u(x_n - x^*) + x^*, \tag{2}$$

where λ_u is the eigenvalue of the unstable manifold e_u , **6)** compute δx , the difference between the predicted next system value \hat{x}_{n+1} , and the desired next system value x_{n+1} (located on the stable manifold) as:

$$\delta x = \left(\frac{\lambda_u}{\lambda_u - 1} \right) \left(\frac{1}{g \cdot f_u} \right) (\xi_n - \xi^*) \cdot f_u, \tag{3}$$

where f_u is the unstable contravariant eigenvector given by $f_u \cdot e_u = 1$ and $f_u \cdot e_s = 0$, and **7)** determine the intervention (i.e., stimulation) time as:

$$x_{n+1} = \hat{x}_{n+1} + \delta x. \tag{4}$$

Note that because g and e_u are estimated quantities, the computation of δx by Eq. (3) does not guarantee that ξ_{n+1} will be placed directly onto e_s via Eq. (4).

B. The SMP control technique

Here, we introduce an alternative to PPF control, called *stable manifold placement* (SMP). We will refer to the SMP and PPF control techniques as PPF-type control techniques, because both techniques place the system’s state point onto the stable manifold of the desired UPO by delivering a perturbation directly to the variable under control. While PPF control uses an OGY-based method for determining the intervention time, SMP control simply computes the desired intervention time directly from the algebraic equation of the stable manifold. Initially, SMP control must estimate (from pre-recorded data): **1)** The UPO ξ^* , and **2)** the stable manifold e_s . Then, at each control intervention [depicted geometrically in Fig. 2(b)], the algorithm only must: **3)** Determine the intervention (i.e., stimulation) time:

$$x_{n+1} = \lambda_s(x_n - x^*) + x^*, \tag{5}$$

where λ_s is the eigenvalue of the stable manifold e_s . Note that, as shown in Figs. 2(a) and (b), the intervention times for PPF control [Eq. (4)] and SMP control [Eq. (5)] are, in principle, the same. However, because SMP control does not rely on estimation of e_u or g , it guarantees (unlike PPF control) that ξ_{n+1} is always computed such that it will be placed directly onto the estimated stable manifold e_s . (With PPF control, estimation errors in e_u or g can lead to intervention-time errors.) Furthermore, the SMP technique requires only two estimations (ξ^* and e_s), compared to the four estimations (ξ^* , e_s , e_u , and g) required by the PPF technique. Thus, SMP control is more robust (because it guarantees that

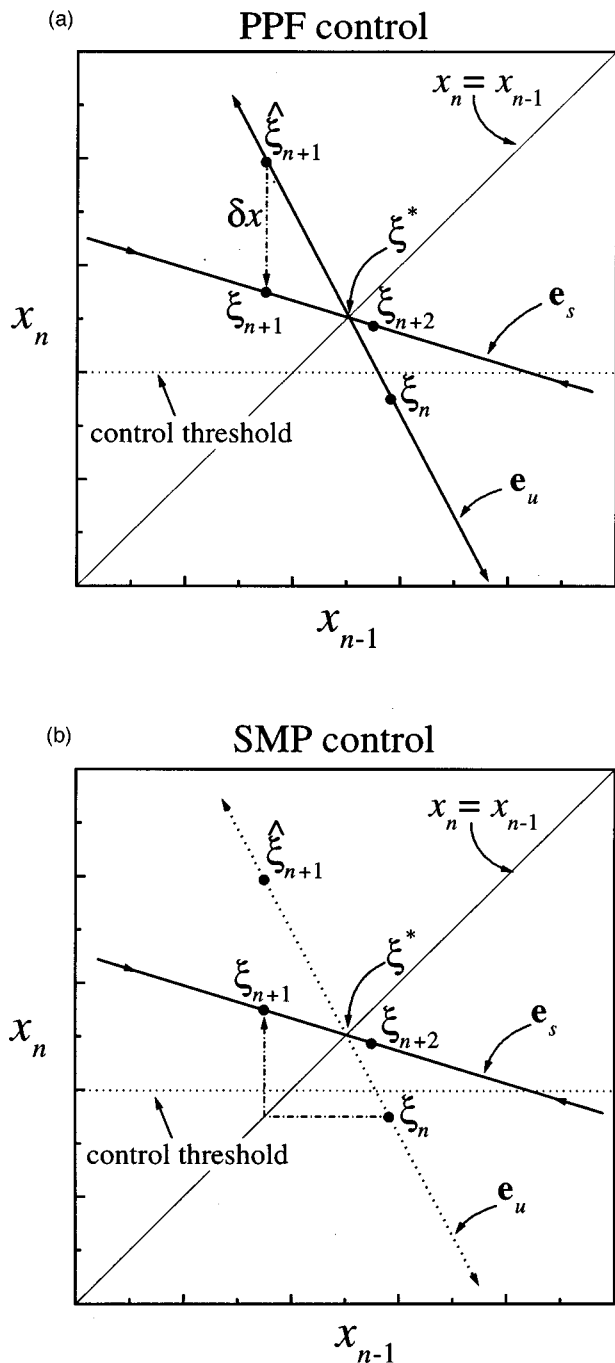


FIG. 2. Geometric depiction of (a) the control perturbation δx required to place ξ_{n+1} onto the estimated stable manifold e_s using the PPF technique, and (b) direct placement of ξ_{n+1} onto the estimated stable manifold e_s using the SMP technique. Provided that the PPF technique correctly estimates g and e_u , the position of ξ_{n+1} will be identical for the two techniques. Note that in (b), the unstable manifold e_u is shown as a dotted line because neither e_u nor ξ_{n+1} is estimated by the SMP technique.

ξ_{n+1} is always placed directly onto e_s) and less computationally intensive (because it requires the estimation of fewer system quantities) than PPF control.

IV. THE DYNAMICS OF PPF-TYPE CONTROL

In addition to the arrhythmic rabbit heart study,¹⁶ the PPF control technique has been used to control irregular in-

terspike intervals (ISIs) from rat hippocampal neuronal networks¹⁷ and the FitzHugh-Nagumo neuronal model.¹⁸ A shortcoming of these previous studies¹⁶⁻¹⁸ is that no distinction was made (in figures depicting control trials) between spontaneous action potentials and those induced via control stimulation. The lack of such a distinction eliminates the possibility of viewing the dynamical results of individual control perturbations, e.g., observing whether a perturbation is followed by the expected stable manifold approach to the UPO. Without such a distinction, it is impossible to determine whether ‘successful’ control is the result of the PPF control technique: **1)** Accomplishing its goal of utilizing system dynamics, **2)** over-stimulating the system such that most (or all) of the action potentials were stimulus-induced (similar to traditional pacing techniques), or **3)** modifying the system dynamics in a manner that lead to interval regularization. A recent study,³¹ which showed that successful control (i.e., stabilization of fluctuations about a nominal interval length) could be achieved with demand pacing of stochastic, as well as deterministic, integrate-and-fire systems, lends further support to the contention that analysis of the dynamical results of individual control perturbations is essential.

To examine the expected dynamics of PPF-type control, we applied SMP control to a simple geometric model of a chaotic system in the linear neighborhood of the UPO. This model represents the system’s state point once it has entered into the linear neighborhood of a given UPO, and thus is not valid for regions of the attractor outside of that neighborhood. Nevertheless, because chaos control techniques are designed for control only within the linear UPO neighborhood, this model is appropriate for the purpose of observing PPF-type control dynamics. In this model, the system’s state point is defined as:

$$\xi_n = [x_{n-1}, x_n]^T. \tag{6}$$

We used the SMP control technique to constrain ξ_n within the linear control region around the period-1 UPO ξ^* , which is characterized by one stable manifold (e_s , with eigenvalue λ_s) and one unstable manifold (e_u , with eigenvalue λ_u). Such dynamics are similar to those reported in the experimental applications of PPF control.^{16,17} This geometric model provides the freedom to vary the UPO location and the manifold eigenvalues, and therefore enables one to test the effectiveness of the control technique for varying system dynamics. With this model, the next system value x_{n+1} is mapped from the current system value x_n according to the equation of an ‘effective’ manifold (e_{eff} , with eigenvalue λ_{eff}):

$$x_{n+1} = \lambda_{eff}(x_n - x^*) + x^* + \zeta_n, \tag{7}$$

where ζ_n is an iterate of a Gaussian white-noise time series with zero mean and standard deviation σ_ζ , and λ_{eff} is given by:

$$\lambda_{eff} = \frac{b\lambda_u + a\lambda_s}{a + b}, \tag{8}$$

where a , as depicted in the schematic of Fig. 3, is the Euclidean distance between ξ_n and e_u , and b is the Euclidean

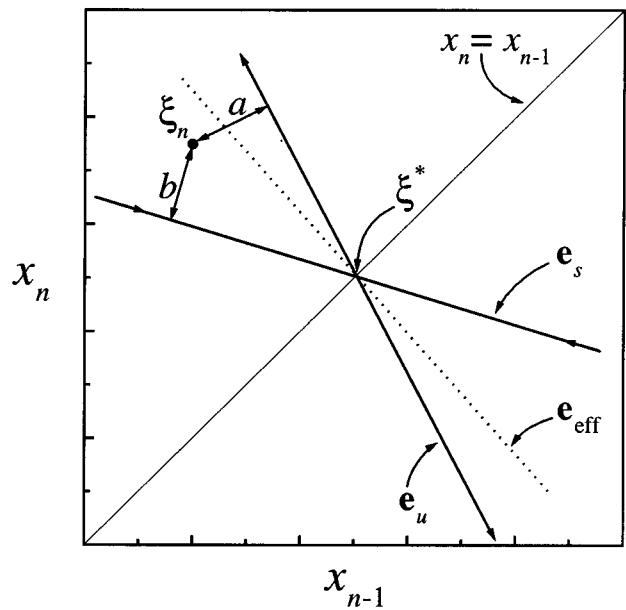


FIG. 3. Schematic first-return map showing the effective manifold e_{eff} for a given state point ξ_n , as modeled in the linear neighborhood of a UPO. a is the Euclidean distance between ξ_n and e_u , and b is the Euclidean distance between ξ_n and e_s .

distance between ξ_n and e_s . The use of such an ‘effective’ manifold to map the state point makes the assumption that the stable and unstable manifolds exert attracting and repelling forces, respectively, on ξ_n that are proportional to their distances from ξ_n .³² Note that if ξ_n lies on the stable or unstable manifold, then the mapping of Eq. (7) is simply the algebraic equation of the stable or unstable manifold. If ξ_n lies between e_s and e_u , as depicted in Fig. 3, then e_{eff} [as computed via Eq. (8)] will not necessarily pass through ξ_n [as in the case depicted in Fig. 3].

For this study, the state point was chosen to start at a random location on the unstable manifold near the UPO. Thus, the mapping of Eq. (7) initially dictated that the state point march away from the UPO at the exponential rate λ_u . The state point was permitted to progress outward along the unstable manifold until ξ_n moved below the control threshold, whereupon an SMP control perturbation was applied. This control perturbation placed the next state point ξ_{n+1} onto the stable manifold according to Eq. (5). From that point, the mapping of Eq. (7) pulled ξ_n toward ξ^* via the stable manifold until the additive noise ζ_n caused Eq. (7) to repel the state point from ξ^* via the unstable manifold. When the state point crossed the control threshold again, it was pulled back onto the stable manifold with an SMP perturbation.

Figure 4(a) shows the first-return map of the first 25 points of a trial with $\lambda_s = -0.25$, $\lambda_u = -1.5$, $\sigma_\zeta = 0.0005$, and $\xi^* = [0.500, 0.500]^T$. Figure 4(a) shows that the state point marched away (on alternate sides) from ξ^* along e_u . When the state point moved below the control threshold, an SMP control intervention that placed the next state point

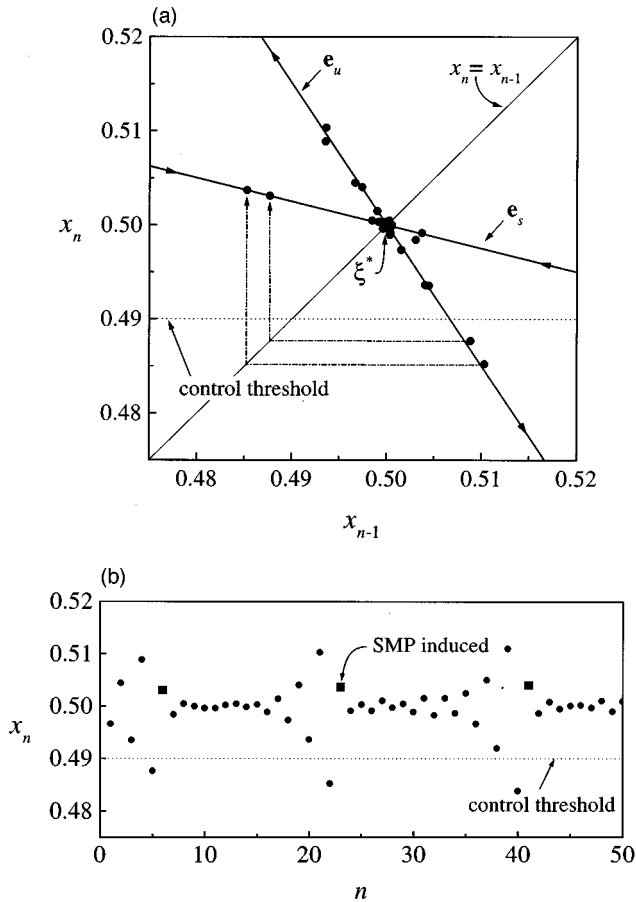


FIG. 4. Geometric depiction of SMP control of a chaotic system in the linear control region around a UPO ξ^* , which is characterized by a stable manifold e_s (with stable eigenvalue $\lambda_s = -0.25$) and an unstable manifold e_u (with unstable eigenvalue $\lambda_u = -1.5$). The system is iterated according to Eq. (7) with $\sigma_\zeta = 0.0005$, and $\xi^* = [0.500, 0.500]^T$. An SMP perturbation [according to Eq. (5)] was introduced whenever x_n crossed below the control threshold ($x = 0.49$). (a) Shows the first-return map of the first 25 intervals x_n of the iterated sequence. (b) Shows the time-domain progression of the first 50 intervals, with SMP perturbation-induced pulses annotated by solid squares.

onto \hat{e}_s was applied. The state point then progressed toward ξ^* until it was repelled via the unstable manifold. This pattern was repeated indefinitely, with quantitative differences between interventions resulting from the additive noise ζ_n . The time-domain depiction of the first 50 points of this sequence is shown in Fig. 4(b). In this depiction, the alternating, exponential divergence from ξ^* along the unstable manifold, followed by an SMP perturbation-induced approach to ξ^* along the stable manifold, can be clearly seen. This dynamical pattern is the expected result of successful PPF-type control.

Figure 5 (where $\lambda_s = -0.25$, $\lambda_u = -1.5$, $\sigma_\zeta = 0.0005$, and $\xi^* = [0.500, 0.500]^T$) illustrates an example of the effects of finite estimation errors, which are invariably associated with experimental preparations. In this example, the real stable manifold e_s and the real UPO ξ^* were misestimated as \tilde{e}_s and $\tilde{\xi}^* = [\tilde{x}^*, \tilde{x}^*]^T = [0.505, 0.505]^T$, respectively. Because of the misestimation, the SMP control perturbations

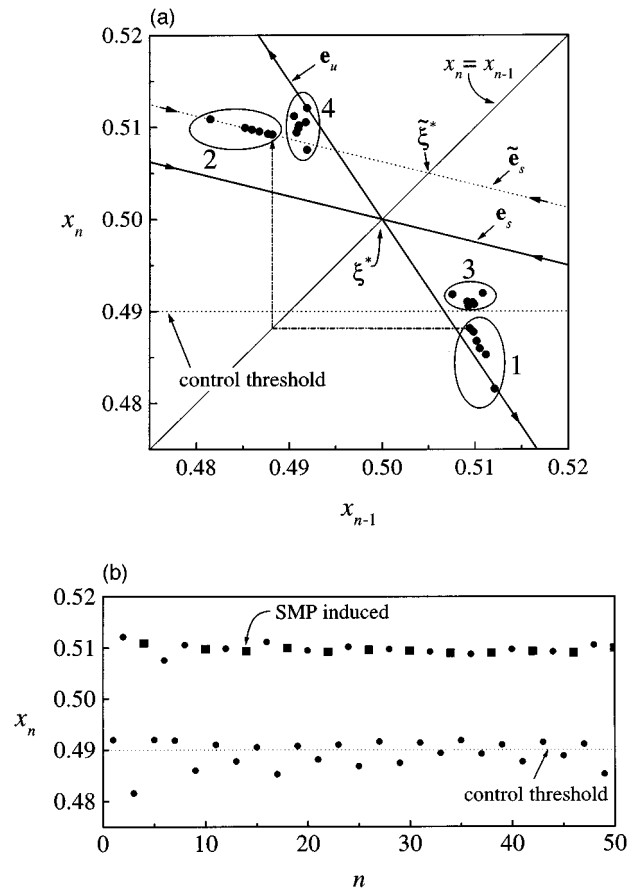


FIG. 5. Geometric depiction of SMP control of a chaotic system in the linear control region around a UPO ξ^* , which is characterized by a stable manifold e_s (with stable eigenvalue $\lambda_s = -0.25$) and an unstable manifold e_u (with unstable eigenvalue $\lambda_u = -1.5$). The system is iterated according to Eq. (7) with $\sigma_\zeta = 0.0005$, and $\xi^* = [0.500, 0.500]^T$. In this trial, the real stable manifold e_s and the real UPO ξ^* were misestimated as \tilde{e}_s and $\tilde{\xi}^* = [\tilde{x}^*, \tilde{x}^*]^T = [0.505, 0.505]^T$, respectively. An SMP perturbation [according to Eq. (9)] was introduced whenever x_n crossed below the control threshold ($x = 0.49$). (a) Shows the first-return map of the first 25 intervals x_n of the iterated sequence. The system was controlled in a ‘quasi’ period-4 rhythm, in which the state point jumped sequentially from regions 1 \rightarrow 2 \rightarrow 3 \rightarrow 4. (b) Shows the time-domain progression of the first 50 intervals, with SMP perturbation-induced pulses annotated by solid squares.

were determined by substituting \tilde{x}^* for x^* in Eq. (5) such that:

$$x_{n+1} = \lambda_s(x_n - \tilde{x}^*) + \tilde{x}^*. \tag{9}$$

In Fig. 5(a) it can be seen that the SMP perturbations placed the state point onto the misestimated stable manifold \tilde{e}_s . After each perturbation, the state point obeyed the ‘real’ mapping of Eq. (7) (i.e., obeying e_s and ξ^* , rather than \tilde{e}_s and $\tilde{\xi}^*$) until it crossed the control threshold and the next SMP perturbation was applied. Due to the misestimation, the state point never approached the UPO as in the ‘successful’ trial depicted in Fig. 4. In fact, the system was controlled in a ‘quasi’ period-4 rhythm, in which the state point jumped sequentially from regions 1 \rightarrow 2 \rightarrow 3 \rightarrow 4 [shown in Fig. 5(a)]. This behavior can be seen in the time-domain depiction of

Fig. 5(b). Additionally, because of the misestimation, more frequent control perturbations were required, compared with the “successful” trial depicted in Fig. 4. The resultant period-4 rhythm is similar to the low-order periods that Garfinkel *et al.*¹⁶ obtained when controlling the irregular rabbit heart tissue. Thus, it is possible that the inability to achieve tight period-1 control in the rabbit heart control experiments¹⁶ may have been the result of small misestimations of the UPO dynamics.

V. CONCLUSIONS

Here we have shown that the SMP technique can be used to stabilize a system that has UPO dynamics that are characterized by one stable manifold and one unstable manifold. Figures 4 and 5 depict the dynamical results of PPF-type control for such a system. These figures demonstrate that if a distinction is made between spontaneous and induced action potentials, there is little ambiguity as to the effectiveness of the control. Additionally, such a presentation of results can be used to illuminate the cause of control failure (as seen in Fig. 5). If the spontaneous and induced firings were differentiated in the three prior applications of PPF control,^{16–18} some of the controversy^{18,19} surrounding these studies may have been avoided. Thus, such a distinction should be made in all future applications of PPF-type control.

There is experimental evidence that model-independent control techniques can be used to eliminate pathological cardiac rhythms.^{16,22} Given the results of the present study and prior experimental applications of PPF control, it may be possible to use PPF-type control techniques to eliminate pathological rhythms in a clinical setting. However, important questions regarding the physiological feasibility of PPF-type control must first be addressed. One issue^{18,19} is whether excitable physiological systems are actually characterized by UPOs with one stable manifold and one unstable manifold (as required by PPF-type control). Another issue is whether the control stimulus significantly modifies the UPO dynamics, i.e., more than simply placing the state point onto the stable manifold. PPF-type control requires that the state point obey the dynamics of the stable manifold once it is placed onto that stable manifold. Thus, it is assumed that the perturbation has no residual effects, i.e., the state point behaves as if it arrived on the stable manifold naturally. As mentioned earlier,²⁵ although a suprathreshold PPF-type stimulus can be a small perturbation to x , the stimulus is a large perturbation to the excitable-system dynamics. Because of this fact, it is not clear that the system dynamics will instantaneously return to those of the unperturbed system (such that the system’s state point will obey the dynamics of the stable manifold) after a PPF-type control perturbation. Further investigation is needed to address these issues and determine whether or not the dynamics of successful PPF-type control, as demonstrated in this modeling study, are physiologically feasible.

ACKNOWLEDGMENTS

This work was supported by the National Science Foundation.

- ¹M. C. Mackey and L. Glass, *Science* **197**, 287 (1977).
- ²L. Glass and M. C. Mackey, *Ann. (N.Y.) Acad. Sci.* **316**, 214 (1979).
- ³M. C. Mackey and J. G. Milton, *Ann. (N.Y.) Acad. Sci.* **504**, 16 (1987).
- ⁴M. R. Guevara, L. Glass, and A. Shrier, *Science* **214**, 1350 (1981).
- ⁵J. Bélair, L. Glass, U. an der Heiden, and J. Milton, *Chaos* **5**, 1 (1995).
- ⁶L. Glass, *Phys. Today* **49**(8), 40 (1996).
- ⁷N. S. Nise, *Control Systems Engineering* (The Benjamin/Cummings Publishing Company, Inc., Redwood City, California, 1992), p. 630.
- ⁸E. Ott, C. Grebogi, and J. A. Yorke, *Phys. Rev. Lett.* **64**, 1196 (1990).
- ⁹W. L. Ditto, S. N. Rauseo, and M. L. Spano, *Phys. Rev. Lett.* **65**, 3211 (1990).
- ¹⁰E. R. Hunt, *Phys. Rev. Lett.* **67**, 1953 (1991).
- ¹¹R. Roy, T. W. Murphy, Jr., T. D. Maier, Z. Gills, and E. R. Hunt, *Phys. Rev. Lett.* **68**, 1259 (1992).
- ¹²V. Petrov, V. Gáspár, J. Masere, and K. Showalter, *Nature (London)* **361**, 240 (1993).
- ¹³B. Hübinger, R. Doerner, W. Martienssen, W. Herdering, R. Pitka, and U. Dressler, *Phys. Rev. E* **50**, 932 (1994).
- ¹⁴R. Jan de Korte, J. C. Schouten, and C. M. van den Bleek, *Phys. Rev. E* **52**, 3358 (1995).
- ¹⁵D. J. Christini, J. J. Collins, and P. S. Linsay, *Phys. Rev. E* **54**, 4824 (1996).
- ¹⁶A. Garfinkel, M. L. Spano, W. L. Ditto, and J. N. Weiss, *Science* **257**, 1230 (1992).
- ¹⁷S. J. Schiff, K. Jerger, D. H. Duong, T. Chang, M. L. Spano, and W. L. Ditto, *Nature (London)* **370**, 615 (1994).
- ¹⁸D. J. Christini and J. J. Collins, *Phys. Rev. Lett.* **75**, 2782 (1995).
- ¹⁹L. Glass and W. Zeng, *Int. J. Bifurcation Chaos* **4**, 1061 (1994).
- ²⁰M. E. Brandt and G. Chen, *Int. J. Bifurcation Chaos* **6**, 715 (1996).
- ²¹D. J. Christini and J. J. Collins, *Phys. Rev. E* **53**, R49 (1996).
- ²²K. Hall, D. J. Christini, M. Tremblay, J. J. Collins, L. Glass, and J. Billette, *Phys. Rev. Lett.* **78**, 4518 (1997).
- ²³Two control techniques (Refs. 19 and 20) that also directly perturb the controlled system variable have been developed for the control of cardiac chaos modeled by a one-dimensional map system. These techniques are only applicable to one-dimensional systems, in contrast to the PPF control technique which is applicable to higher dimensional systems.
- ²⁴Recently, an OGY-type control technique has been used to control a pathological cardiac rhythm in a numerical model (Ref. 21) and in an *in vitro* rabbit heart preparation (Ref. 22).
- ²⁵For PPF control, it is important to draw a distinction between the suprathreshold stimulus and the perturbation. The stimulus is clearly a large perturbation to the action-potential dynamics (as noted in Ref. 19); however, the PPF perturbation (δx) can be quite small.
- ²⁶With demand pacing, stimuli are used to prevent x from exceeding some pre-determined value. See: M. R. Neumann, in *Medical Instrumentation Application and Design*, 2nd ed., edited by J. G. Webster (Houghton Mifflin, Boston, 1992), pp. 699–700.
- ²⁷D. Pierson and F. Moss, *Phys. Rev. Lett.* **75**, 2124 (1995).
- ²⁸X. Pei and F. Moss, *Nature (London)* **379**, 618 (1996).
- ²⁹P. So, E. Ott, S. J. Schiff, D. T. Kaplan, T. Sauer, and C. Grebogi, *Phys. Rev. Lett.* **76**, 4705 (1996).
- ³⁰D. T. Kaplan, *Physica D* **73**, 38 (1994).
- ³¹T. Sauer, *Fields Inst. Commun.* **11**, 63 (1997).
- ³²Note that the results of this study are not dependent on the assumption of a linear relationship between manifold force (on ξ_n) and the distance from the manifold. Equation (7) simply provides a method for mapping ξ_n when it does not lie exactly on e_s or e_u .
- ³³UPOs appear as unstable periodic fixed points on a first-return map.